

See discussions, stats, and author profiles for this publication at: <https://www.researchgate.net/publication/237839298>

Chalcogen-Based Aerogels As Sorbents for Radionuclide Remediation

ARTICLE *in* ENVIRONMENTAL SCIENCE & TECHNOLOGY · JUNE 2013

Impact Factor: 5.33 · DOI: 10.1021/es400595z · Source: PubMed

CITATIONS

24

READS

73

9 AUTHORS, INCLUDING:



[Brian J. Riley](#)

Pacific Northwest National Laboratory

96 PUBLICATIONS 695 CITATIONS

[SEE PROFILE](#)



[Wooyong Um](#)

Pacific Northwest National Laboratory

91 PUBLICATIONS 799 CITATIONS

[SEE PROFILE](#)



[William C. Lepry](#)

McGill University

16 PUBLICATIONS 55 CITATIONS

[SEE PROFILE](#)

Chalcogen-Based Aerogels As Sorbents for Radionuclide Remediation

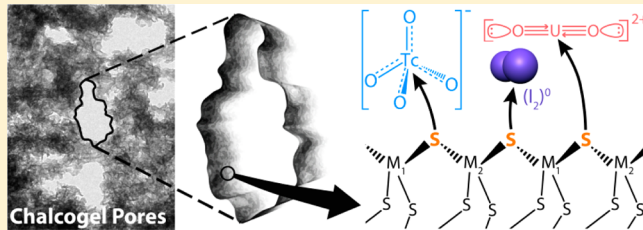
Brian J. Riley,^{*,†} Jaehun Chun,[†] Wooyong Um,[†] William C. Lepry,[†] Josef Matyas,[†] Matthew J. Olszta,[†] Xiaohong Li,[‡] Kyriaki Polychronopoulou,[‡] and Mercouri G. Kanatzidis[‡]

[†]Pacific Northwest National Laboratory, Richland, Washington 99352, United States

[‡]Department of Chemistry, Northwestern University, Evanston, Illinois 60208, United States

Supporting Information

ABSTRACT: The efficient capture of radionuclides with long half-lives such as technetium-99 (⁹⁹Tc), uranium-238 (²³⁸U), and iodine-129 (¹²⁹I) is pivotal to prevent their transport into groundwater and/or release into the atmosphere. While different sorbents have been considered for capturing each of them, in the current work, nanostructured chalcogen-based aerogels called chalcogels are shown to be very effective at capturing ionic forms of ⁹⁹Tc and ²³⁸U, as well as nonradioactive gaseous iodine (i.e., a surrogate for ¹²⁹I₂), irrespective of the sorbent polarity. The chalcogel chemistries studied were Co_{0.7}Bi_{0.3}MoS₄, Co_{0.7}Cr_{0.3}MoS₄, Co_{0.5}Ni_{0.5}MoS₄, PtGe₂S₅, and Sn₂S₃. The PtGe₂S₅ sorbent performed the best overall with capture efficiencies of 98.0% and 99.4% for ⁹⁹Tc and ²³⁸U, respectively, and >99.0% for I₂(g) over the duration of the experiment. The capture efficiencies for ⁹⁹Tc and ²³⁸U varied between the different sorbents, ranging from 57.3–98.0% and 68.1–99.4%, respectively. All chalcogels showed >99.0% capture efficiency for iodine over the test duration. This versatile nature of chalcogels can provide an attractive option for the environmental remediation of the radionuclides associated with legacy wastes from nuclear weapons production as well as wastes generated during nuclear power production or nuclear fuel reprocessing.



INTRODUCTION

Aerogels are highly porous semisolids with many emerging applications. The most commonly studied types of aerogels are silica-based aerogels but other types have been pursued. One such type are nonoxide aerogels called *chalcogels* that are composed of chalcogen (S, Se, and/or Te)-based moieties and often have different properties than their oxide-based analogs.¹ Chalcogels can be prepared through a few different methods including (1) thiolytic of alkoxides with H₂S (e.g., GeS_x),² (2) condensation/agglomeration of nanoparticles (e.g., CdS, ZnS, CdSe, and PbS),³ or (3) chemical linkage of chalcogenide clusters with interlinking metals.^{4,5} Routes (1) and (2) pose limitations where route (1) typically requires the use of the highly toxic gas H₂S and the compositions for route (2) are restricted to available nanoparticle chemistries. Route (3) is a more attractive option mainly because of the vast compositional flexibility. To date, Ge–S, Ge–Se, Sn–S, Sn–Se, Mo–S, W–S, and Fe–S precursor building blocks have been identified and these precursors undergo gelation when combined with one or more interlinking metal ions from a growing list that includes Bi³⁺, Co²⁺, Ni²⁺, Sb³⁺, Sn²⁺, and Zn²⁺.^{4–11}

A key feature of chalcogels is that they can be used to selectively capture gaseous and ionic species, some of which may be desirable for separations and environmental remediation.^{4–12} This “built-in” selectivity, as it is best understood, is at least partially based on the affinity between the species of interest and the elementary building blocks of the chalcogels via

the chemical hardness (η , in eV) and the polarizability. Pearson’s Hard–Soft Acid–Base (HSAB) principle^{13–15} uses the chemical hardness of species to classify them as hard or soft Lewis acids or bases as

$$\eta = \frac{1}{2}(I - A) \quad (1)$$

where I is the ionization energy (in eV) and A is the electron affinity (in eV) of a species. This relation can be used to predict the affinity of any species of interest for another as long as these data are available. From eq 1, it can be determined that the chalcogens, S ($\eta = 4.12$ eV), Se ($\eta = 3.86$ eV), and Te ($\eta = 3.52$ eV), are soft Lewis bases.¹³ Some heavy metal ions are soft Lewis acids and tend to bind well to chalcogels showing potential for environmental remediation,^{4,10–12} for example, Hg²⁺ ($\eta = 7.7$ eV), Pb²⁺ ($\eta = 8.5$ eV), and Cd²⁺ ($\eta = 10.3$ eV).¹³ Also, chalcogels have been demonstrated to have a selective affinity for certain gases such as the ranking H₂ < CH₄ < CO₂ < C₂H₆ for PtGeS and PtSbGeSe chalcogels, where the higher affinities were attributed to the more polarizable molecules.⁷

However, chalcogel affinity for radionuclides has never been explored until now while a limited study with nonradioactive

Received: February 5, 2013

Revised: April 26, 2013

Accepted: May 17, 2013

Published: June 13, 2013



Table 1. Summary of Chalcogel Recipes

| chalcogel | precursor 1 (g in mL) | precursor 2 (g in mL) | precursor 3 (g in mL) | solvent | gelation time (days) |
|--|--|--|---|-----------|----------------------|
| CoBiMoS (Co _{0.7} Bi _{0.3} MoS ₄) | Co(NO ₃) ₂ ·6H ₂ O (3.34 g in 66 mL) | Bi(CH ₃ COO) ₃ (1.27 g in 66 mL) | (NH ₄) ₂ MoS ₄ (4.29 g in 66 mL) | formamide | 14 |
| CoCrMoS (Co _{0.7} Cr _{0.3} MoS ₄) | Co(NO ₃) ₂ ·6H ₂ O (3.34 g in 66 mL) | Cr(NO ₃) ₃ ·9H ₂ O (1.32 g in 66 mL) | (NH ₄) ₂ MoS ₄ (4.29 g in 66 mL) | formamide | 12 |
| CoNiMoS (Co _{0.5} Ni _{0.5} MoS ₄) | CoCl ₂ ·6H ₂ O (0.143 g in 7.5 mL) | Ni(NO ₃) ₂ ·6H ₂ O (0.175 g in 7.5 mL) | (NH ₄) ₂ MoS ₄ (0.312 g in 15 mL) | formamide | 28 |
| PtGeS (PtGe ₂ S ₅) | ((CH ₃) ₄ N) ₄ Ge ₄ S ₁₀ (1.09 g in 36 mL) | K ₂ PtCl ₄ (0.995 g in 24 mL) | N/A | DIW | 17 |
| SnS (Sn ₂ S ₃) | Na ₄ Sn ₂ S ₆ ·14H ₂ O (3.10 g in 80 mL) | Sn(CH ₃ COO) ₂ (1.89 g in 80 mL) | N/A | formamide | 37 |

iodine was reported.¹¹ This study evaluates the capture efficiency of chalcogels for technetium (⁹⁹Tc), uranium (²³⁸U) and iodine. The target iodine is ¹²⁹I evolved as a gaseous species (¹²⁹I₂(g)), although nonradioactive iodine was used in these studies. All three of these radionuclides are associated with legacy wastes (i.e., weapons production) as well as nuclear power production and nuclear fuel reprocessing. All of these have very long half-lives (*t*_{1/2}) of 2.1 × 10⁵ y (⁹⁹Tc), 4.5 × 10⁹ y (²³⁸U), and 1.6 × 10⁷ y (¹²⁹I) so their releases must fall below regulatory limits^{16,17} because they pose serious concerns toward public health in the event that they are leached into the groundwater and/or are released into the atmosphere.^{18,19} This has triggered significant research interest for the development of sorbents that can effectively and selectively capture these species out from the other species within their proximity, some of which might be nonhazardous.

Both ⁹⁹Tc and ¹²⁹I are volatile and tend to leave as off-gases during high temperature processes such as vitrification for waste disposal or voloxidation for nuclear fuel reprocessing.²⁰ The ⁹⁹Tc will likely be reoxidized and converted to the pertechnetate anion (TcO₄⁻) once being exposed to oxygen, so ⁹⁹Tc exists as TcO₄⁻ in solution at most pH conditions. The mobility of TcO₄⁻ in subsurface water is fairly significant; it would not be mitigated by sorption or solubility limitations.²¹ Several different types of sorbents have been investigated for capturing Tc that include ion-exchange materials,²² activated carbon,²³ and natural minerals such as bentonite²⁴ and goethite.¹⁸

On the other hand, ¹²⁹I typically exists as iodide or iodate species upon introduction into aqueous solution. Due to the high vapor pressure and adverse health effects of gaseous iodine, the Environmental Protection Agency (EPA) regulation 40 CFR 190 requires more than 99.4 mass% for ¹²⁹I capture and immobilization.¹⁶ Many different iodine sorbents have been identified that include chalcogels,¹¹ silver-functionalized silica aerogels,²⁵ apatite mineral structures,²⁶ metal–organic frameworks²⁷ and monolithic aerogels of polymeric organic framework.²⁸ The most prevalent iodine sorbent studied in the United States is a silver-exchanged zeolite (AgZ), while the Japanese and Europeans have studied AgNO₃-impregnated alumina and silica.²⁹ The AgZ and AgNO₃-impregnated sorbents require silver to bind I₂(g) but have an advantage in that they can be prepared in large volumes.

The most prevalent form of U in the legacy waste is the hexavalent form (i.e., uranyl or UO₂²⁺).¹⁹ While UO₂(OH)₂⁺, UO₂(OH)₃⁻, and UO₂(CO₃)₂²⁻ species are dominant with increasing pH in solution within the presence of the carbonate ion,³⁰ UO₂²⁺ exists under oxidizing conditions and is considered as stable ionic form of U under low pH conditions.³¹ Some of the U sorbents that have been studied include silica gels,³² activated carbon-silica aerogel composite

materials,³³ and partially sintered silica aerogels.³⁴ Additionally, work has been done with a porous metal sulfide, K₂MnSn₂S₆ (KMS-1) looking to capture U from seawater where the capture mechanism is believed to be an ion exchange process where UO₂²⁺ ions substitute into the crystal structure for the K⁺ ions.³⁵

The purpose of the current study was to extend the previous sorbent work¹¹ with chalcogels to study their efficacy for radionuclides. In this study, five different chalcogel chemistries were evaluated for capture of 10⁻⁶ M UO₂²⁺, 10⁻⁶ M TcO₄⁻, and 4.2 ppm iodine gas (by volume). The chalcogel chemistries studied were Co_{0.7}Bi_{0.3}MoS₄ (CoBiMoS), Co_{0.7}Cr_{0.3}MoS₄ (CoCrMoS), Co_{0.5}Ni_{0.5}MoS₄ (CoNiMoS), PtGe₂S₅ (PtGeS), and Sn₂S₃ (SnS).

EXPERIMENTAL SECTION

2.1. Chalcogel Fabrication. All chalcogels were prepared with techniques discussed in the literature.^{4,6,7,9,11} For each chalcogel, different chemical precursors were dissolved separately in a solvent (i.e., deionized water (DIW) or formamide), mixed together, and left to gel over a period of time (Table 1). The Na₄Sn₂S₆·14H₂O precursor for making the SnS chalcogel was prepared as shown in previous studies^{10,36} with Na₂S·9H₂O and SnCl₄·5H₂O as starting materials. The ((CH₃)₄N)₄Ge₄S₁₀ precursor for the PtGeS chalcogel was prepared in a hydrothermal reaction according to literature procedures with (CH₃)₄NOH, Ge, and S as starting materials.^{11,37} The Bi(CH₃COO)₃, Co(NO₃)₂·6H₂O, CoCl₂·6H₂O, Cr(NO₃)₃·9H₂O, K₂PtCl₄, (NH₄)₂MoS₄, Ni(NO₃)₂·6H₂O, and Sn(CH₃COO)₂ precursors were purchased commercially (see Table S1 in the Supporting Information (SI) for the purity and vendor of each chemical precursor). For each chalcogel, the individual precursors were added to solvents in separate beakers and stirred until the precursors were dissolved. Then, they were combined, stirred for a few minutes, and cast into either glass or polypropylene vials with lids and left to undergo gelation.

Following gelation, the chalcogels were removed from their vials and diced into smaller pieces (~1–5 mm in size) that we call “granules”. All chalcogels were placed into either pure ethanol or a mixture of ethanol and DIW to undergo aging for 1–3 days (see Table S2 in the SI). The aging process was followed by several rinses in a fresh solution of DIW (for PtGeS) or a mixture of ethanol and DIW (all except PtGeS) to remove the water-soluble byproducts of the chemical reactions. This was followed by several washes in 100% ethanol to remove the water. Then, the gels were washed several times with fresh liquid CO₂ in an autoclave to remove the ethanol. Following the rinsing with liquid CO₂, the vessel was heated to take the CO₂ supercritical at which point the CO₂ was slowly vented as a gas.

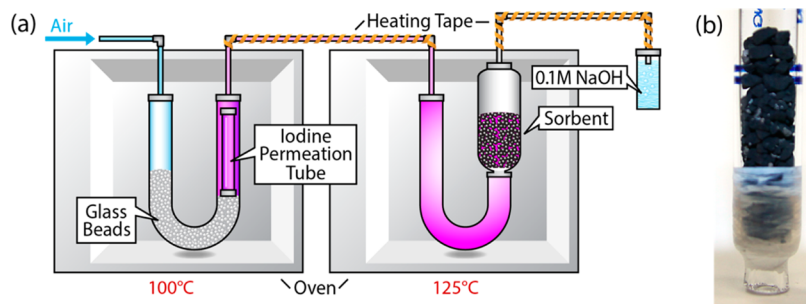


Figure 1. A schematic of the experimental setup for iodine gas uptake test in flowing air containing $I_2(g)$ at 4.2 ppm (a) and a photograph of a CoNiMoS chalcogel (black) in the bottom of the pipet prior to an experiment (b).

In a separate experiment, a series of SnS gels were prepared with the same procedure as those previously described but were not dried with supercritical CO_2 . Instead, the ethanol at the final solvent exchange step was intentionally allowed to evaporate, collapsing the pore structure. The product of this experiment was a SnS xerogel with significantly reduced surface area as compared to the aerogel.

2.2. Characterization. Prior to any uptake experiments, the chalcogels were characterized with a number of different techniques that included specific surface area measurements, scanning electron microscopy (SEM), transmission electron microscopy (TEM), and selected area diffraction (SAD). Specific surface areas were measured for all of the chalcogels with $N_2(g)$ adsorption and desorption isotherms collected with a Quantachrome Autosorb-6B (Quantachrome Instruments, Boynton Beach, FL) gas sorption system on degassed samples. Samples were loaded in a glass sample holder and degassed at different temperatures (25–125 °C) while under vacuum. The degassed samples were analyzed with nitrogen adsorption and desorption at a constant temperature of 77.4 K (−195.75 °C), the temperature of liquid nitrogen. The specific surface areas were determined from the isotherm with the Brunauer–Emmett–Teller (BET) method.³⁸ The Barrett–Joyner–Halenda (BJH) method was also used for the porosity and pore size analyses.³⁹

In order to relate the surface area of the chalcogels to the more common silica aerogels, the “silica equivalent specific surface area” (SSA_{eq}) was calculated.⁵ Here, the chalcogel composition was normalized to SiO_2 having 2 oxygens. For example, $Sn_{2.00}S_{3.00}$ becomes $Sn_{1.33}S_{2.00}$ and the molecular mass of this compound (222.41 g/mol) is compared to that of SiO_2 (60.08 g/mol) and the silica equivalent specific surface area translates to 3.70 times the values measured with the isotherms.

Uncoated chalcogels were analyzed with a JSM-7001F SEM (JEOL USA, Inc., Peabody, MA) in Gentle Beam mode at low acceleration voltage (0.3 kV). Additionally, all chalcogels were analyzed with TEM and SAD with a JEOL 2010F operated at 200 kV with a 50 μm diameter condenser aperture. Powders of each sample were passed through a 325 μm mesh sieve, dispersed in isopropanol, and crushed in an agate mortar and pestle. Lacey carbon copper grids were then passed through the solution to collect fine particles and the grid was allowed to dry.

Regions of interest were identified at electron transparent edges of the crushed powders as to not induce phase separation through beam damage. Bright field and diffraction images were collected from each sample. The microscope was calibrated in diffraction mode with the objective aperture as a physical constant and subsequent selected area diffraction on the aerogels was performed with a selected area aperture (which

highlighted the ~500–700 nm diameter region) with the diffraction pattern focused at the same plane as the objective aperture for consistency.

2.3. Tc and U Capture. For the ^{99}Tc and ^{238}U sorption experiments, masses of ~0.05–0.1 g of the five different chalcogel chemistries were added to separate vials containing 9 mL of DIW (Table S3, SI). In addition, a “blank” sample was also prepared under the same conditions with 9 mL of DIW in a vial without any chalcogel sorbent to monitor radionuclides removal by the vials. Then, 1 mL of a stock solution containing either 10^{-5} M ^{99}Tc (TcO_4^- added as $NaTcO_4$) or 10^{-5} M ^{238}U (UO_2^{2+} added as $UO_2(NO_3)_2$) in DIW was added to the 9 mL vial for a final concentration of 10^{-6} M for each radionuclide. These samples were mixed in the vials for 7 days with an end-over-end rotator and the supernatant was collected after separation of solution with 0.45 μm syringe filter.

The concentration of either ^{99}Tc or ^{238}U in solution after 7 days was measured with inductively coupled plasma mass spectrometry (ICP-MS). The capture efficiency, based on the fraction removed, was calculated with eq 2 where C_o was the initial mass concentration of the radionuclide (^{99}Tc or ^{238}U) and C_f was the final mass concentration of each radionuclide in chalcogel samples after 7 days. Also, the K_d (distribution coefficient) values were determined by comparing the concentrations of ^{99}Tc or ^{238}U between initial and final chalcogel samples as shown in eq 3 where $V = 10$ mL and m was the mass (g) of chalcogel sample used (Table S3, SI).

$$\% \text{efficiency} = 100 \times (C_o - C_f)/C_o \quad (2)$$

$$K_d = V/m \times ((C_o - C_f)/C_f) \quad (3)$$

2.4. Iodine Gas Capture. A schematic of the experimental setup used for the iodine capture experiments is shown in Figure 1 (more details are presented elsewhere²⁵). In this apparatus, air was flowed through a column into an oven at 100 °C and then through a DYNACAL iodine permeation tube with a permeation rate of 22.8597 ng s⁻¹, equating to 4.2 ppm (by volume) $I_2(g)$ in air. The column transported this mixture of air/ $I_2(g)$ into a second oven at 125 °C where the sample holder, a 10 mL glass pipet, was attached to the column. After passing through the pipet, either empty or containing the sorbent, the gas mixture was bubbled through a 0.1 M NaOH scrubber solution in DIW. Calibration runs were performed without a sorbent in the sample holder to determine the flow rate of $I_2(g)$ through the column. During the test, the scrubber solution was periodically removed and replaced with a fresh solution. Then, 20 mL aliquots were analyzed with ICP-MS and the iodine evolution rate was determined in the form of $\mu g L^{-1} s^{-1}$.

Then, 1–5 mL of chalcogel granules were lightly packed into the sample holder and connected to the apparatus in the oven at 125 °C for several hours. The scrubber solutions were collected at different evolution times and analyzed with ICP-MS to determine the concentration of iodine in the sample (C_s). The breakthrough iodine from the experiments with the sorbent in the column was compared to the calibration runs and the capture efficiency of the sorbent was determined with eq 4 where C_c was the iodine concentration calculated from the calibration runs (without sorbent) for the same evolution time.

$$\% \text{efficiency} = 100 \times (C_c - C_s)/C_c \quad (4)$$

RESULTS AND DISCUSSION

3.1. Chalcogel Characterization. The basic microstructure of the SnS chalcogel as observed with SEM is shown in Figure 2. The structure as observed with TEM is

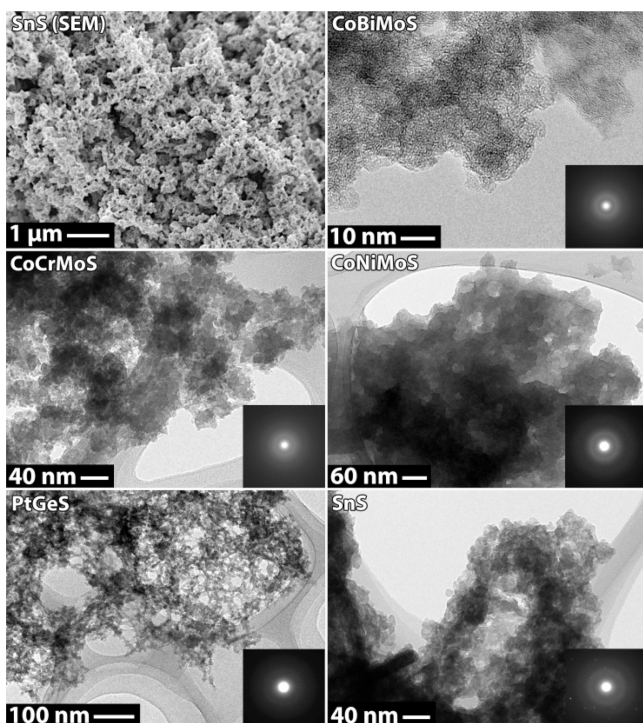


Figure 2. SEM and TEM micrographs of the chalcogels. Insets are SAD patterns showing diffuse scattering consistent with the non-periodic nature of the chalcogels.

presented in Figure 2 and shows noticeably different morphologies between the various chalcogels. The CoBiMoS, CoCrMoS, and CoNiMoS chalcogels looked similar to one another with more dense networks, while the SnS chalcogel showed a more dispersed network and the PtGeS was highly porous. The SAD analysis on representative chalcogel granules showed amorphous structure (Figure 2). Some crystalline diffraction was observed with SnS and is presumed to be surface oxidation as evidenced by white discoloration on the surface of the granules.

The specific surface areas varied significantly with chemistry and, for some of the chalcogels, it also moderately varied with degas temperatures (see Table 2). The CoBiMoS and CoCrMoS chalcogels were tested as powders and it is likely that all of the solvent was removed during the supercritical drying process so the specific surface area was not altered

during heating by desorption of residual solvent. The other three chalcogels (CoNiMoS, PtGeS, and SnS) were analyzed as granules and the general trend was a decrease in specific surface area with increased degas temperatures. This can be attributed to additional pore collapse during heating due to the evaporation of residual solvent; it was fairly difficult to remove all of the solvent during the solvent exchange procedure as was evidenced by minor volumetric reduction of all granules in the weeks following the supercritical CO₂ drying process.

3.2. Tc and U Capture. The sample mass, final solution pH, and solution color varied for each experiment as presented in Figure 3 and the SI. It should be noted that no significant removal (<1%) of each radionuclide was observed on the walls of the glass vials. The Tc and U capture efficiencies varied over the range of chalcogel materials studied (Table 3). The CoBiMoS, PtGeS, and SnS chalcogels showed high removal efficiencies for both ⁹⁹Tc and ²³⁸U at ≥87.3% fractional uptake whereas the CoCrMoS showed the lowest capture efficiencies for ⁹⁹Tc (57.3%) and ²³⁸U (68.1%). The CoNiMoS chalcogel showed low capture efficiency for ⁹⁹Tc (62.2%), but ²³⁸U removal (88.2%) was much higher. With the exception of the CoNiMoS chalcogel, the capture efficiencies of ⁹⁹Tc and ²³⁸U for a given chalcogel were similar (within ~ ± 5%). Note that the K_{ds} for ²³⁸U on CoBiMoS (low pH), CoCrMoS (low pH), and CoNiMoS (high pH) were still higher compared to other sorbents under similar pH conditions.^{40,41}

Typically, surface charges of solid sorbents change with pH conditions in solution because of the amphoteric nature of solid sorbents; the performance of a sorbent (e.g., an ion-exchanging sorbent) is expected to be dependent on the pH, when an affinity between the sorbent and sorbate originates from a polarity difference. That is, an anionic TcO₄⁻ species without any reductant applied is expected to show the highest K_d value at low pH in which positively charged surface sorption sites are dominant, while negatively charged surface sites become predominant and the K_d value decreases as pH increases. However, this is clearly not the case with the chalcogels. As is shown in Table 3, while chalcogels of CoBiMoS and CoCrMoS (or CoNiMoS) showed a decreasing trend of ⁹⁹Tc K_d s with increasing pH, the PtGeS and SnS chalcogels showed higher ⁹⁹Tc K_d values than those of Co-based chalcogels even at higher pH condition. With similar reasoning, the K_{ds} of ²³⁸U sorption should increase with pH because UO₂²⁺ mainly exists under low pH (i.e., positive polarity).⁴² However, a clear correlation cannot be drawn from this data considering that the efficiency of CoBiMoS (pH 2.26) is much higher than that of CoCrMoS (pH 2.72).

3.3. Iodine Gas Capture. The results of the iodine gas capture experiments are summarized in Figure 4a. All of the chalcogels showed very high capture efficiencies of >99% for iodine gas over the duration presented. The MoCoNiS chalcogel showed some breakthrough after the 4 h time point, where uncaptured iodine was measured in the scrubber solution. The reason for this remains unclear. Note that only the SnS chalcogel had a capture efficiency greater than that required to meet the EPA guideline of ≥99.4% for the entire duration of the experiment.¹⁶

The SnS xerogel had a specific surface area of 0.14 m²/g, more than 3 orders of magnitude less surface area than the compositionally equivalent SnS aerogel (456 m²/g) but, surprisingly, showed measurable capture efficiency (Figure 4b). Such appreciable capture efficiency of the xerogel clearly supports the postulation that the affinity between I₂(g) and S

Table 2. Summary of Specific Surface Area (SSA, m^2/g) Measurements, The Calculated Silica Equivalent Surface Area (SSA_{eq} , in Parentheses), and Pore Volume (cm^3/g) for the Various Chalcogels Collected at Different Degassing Temperatures (T_d)

| T_d = chalcogel | 25 °C | | 60 °C | | 100 °C | | 125 °C | |
|--------------------|--|--|--|--|--|--|--|--|
| | SSA, m^2/g (SSA_{eq} , m^2/g) | V_{pore} (cm^3/g) | SSA, m^2/g (SSA_{eq} , m^2/g) | V_{pore} (cm^3/g) | SSA, m^2/g (SSA_{eq} , m^2/g) | V_{pore} (cm^3/g) | SSA, m^2/g (SSA_{eq} , m^2/g) | V_{pore} (cm^3/g) |
| CoBiMoS | 251 (685) | 1.2 | 257 (702) | 1.1 | 255 (696) | 1.1 | 252 (688) | 0.99 |
| CoCrMoS | 118 (276) | 0.69 | 127 (297) | 0.77 | 130 (304) | 0.68 | 132 (309) | 0.78 |
| CoNiMoS | 582 (1371) | 3.0 | 580 (1366) | 3.3 | 551 (1298) | 2.6 | 503 (1185) | 2.2 |
| PtGeS ^a | 423 (1410) | 3.1 | 491 (1636) | 3.4 | 418 (1393) | 2.9 | 428 (1426) | 3.0 |
| SnS | 456 (1688) | 3.9 | 432 (1599) | 3.5 | 378 (1399) | 3.0 | 364 (1347) | 2.2 |

^aThis is data from a different, but identically made and processed, PtGeS sample, presented in our earlier work.¹¹



Figure 3. Pictures of vials containing the various chalcogels in 10 mL of DIW (colors representative of the ^{238}U experiments).

would be a more decisive factor for effective capture than the surface area of a chalcogel.

3.4. Capture Mechanism. Figure 5 shows an inverse relationship between the available surface area and the capture efficiency for the ^{99}Tc and ^{238}U experiments, where the “available surface area” is the product of (1) the sorbent mass added to each solution and (2) the specific surface area (see Table 2 and Table S3 in the SI). The data show a somewhat counterintuitive trend based on a simple rationale for adsorption where the quantity of adsorbed species should be proportional to the available binding sites. Figure 5 suggests that the available surface area and pore volume might not be as critical to maximize the binding efficiency as was previously thought. The fact that the degrees of the inverse correlation differ from the sorbates would also support this rationale. Furthermore, as pointed out, the polarity also cannot explain the trend across different pH values (Table 2).

Regarding iodine capture, all of the chalcogels studied here showed comparably high capture efficiencies. It is known that $\text{I}_2(\text{g})$ is a soft Lewis acid ($\eta = 3.4 \text{ eV}$)¹¹ and since the only common chemistry link between the three sorbents tested is

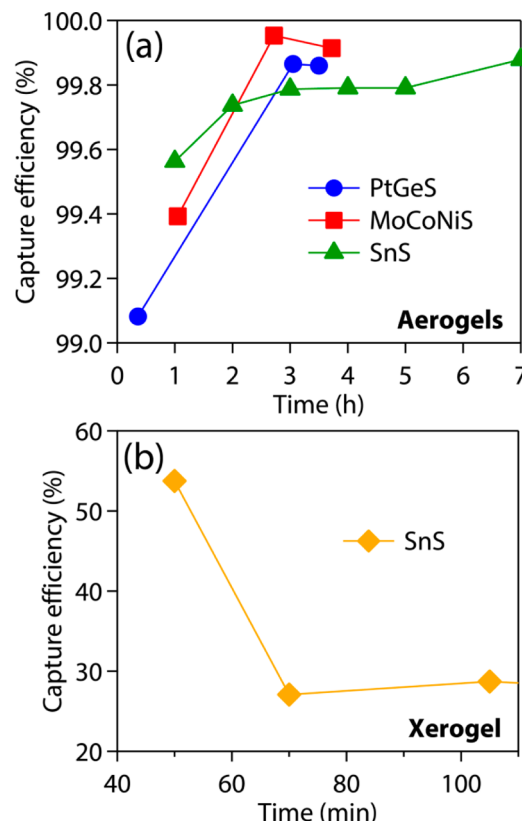


Figure 4. Iodine uptake results for (a) three of the aerogels and (b) a SnS xerogel. Data for PtGeS was extracted from Riley et al.¹¹.

Table 3. Summary of ^{99}Tc and ^{238}U Uptake with Various Chalcogels

| sample ID | ^{99}Tc -uptake | | | | ^{238}U -uptake | | | |
|-----------|--------------------------|--------------------|----------|----------------|--------------------------|--------------------|----------|----------------|
| | eff. (%) | K_d (mL/g) | final pH | color | eff. (%) | K_d (mL/g) | final pH | color |
| CoBiMoS | 94.0 | 1.68×10^3 | 2.31 | very blue | 94.9 | 1.81×10^3 | 2.26 | faintly blue |
| CoCrMoS | 57.3 | 2.88×10^2 | 2.78 | faintly pink | 68.1 | 3.15×10^2 | 2.72 | barely pinkish |
| CoNiMoS | 62.2 | 1.62×10^2 | 4.12 | pale blue | 88.2 | 8.08×10^2 | 9.06 | pale blue |
| PtGeS | 98.0 | 3.61×10^4 | 4.80 | faintly orange | 99.4 | 9.43×10^4 | 4.44 | faintly orange |
| SnS | 87.3 | 1.49×10^3 | 5.47 | faint yellow | 99.1 | 2.31×10^4 | 5.53 | faintly yellow |
| Blank | | | 5.59 | clear | | | 5.18 | clear |

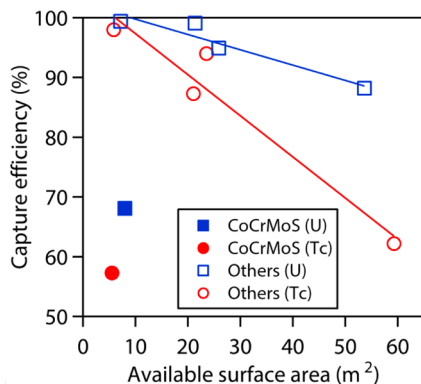


Figure 5. Comparison of capture efficiency (%) for ^{238}U and ^{99}Tc versus available surface area for all chalcogels.

the chalcogen backbone, this seems to suggest a similar binding mechanism between the sorbents and supports the HSAB principle theory. While the UO_2^{2+} ion has been assumed to be a hard Lewis acid, a recent study strongly suggested that the UO_2^{2+} ion is indeed much softer.³⁵ The conventional thinking regarding this ion is that it is a hard ion (hard Lewis acid) because the U is in the 6+ oxidation state. The two double bonds to the oxide ions ($\text{O}=\text{U}=\text{O}$), however, considerably soften the U center and cause it to behave more like a lead ion, providing evidence to support the HSAB principle binding theory. However, while chalcogels do show a selective affinity for softer acids and more polarizable species,^{4–10} based on the wide range of capture efficiencies with the ^{99}Tc and ^{238}U experiments, the HSAB principle alone might not be adequate to explain the binding mechanism for these species. That is because it suggests that the chalcogens, alone, are responsible for binding the species of interest. This warrants further investigations that are currently underway.

3.5. Additional Applications. In addition to the species discussed here (i.e., Hg^{2+} , Pb^{2+} , and Cd^{2+}), chalcogels have been demonstrated to capture other, nonradioactive species^{4,10,12} such as Fe^{2+} ($\eta = 7.3 \text{ eV}$) and Cu^{2+} ($\eta = 8.3 \text{ eV}$).¹³ Based on the HSAB principle as a predictive tool, other soft Lewis acids that could be of interest in ionic form include Pu^{3+} ($\eta = 6.5 \text{ eV}$),⁴³ Am^{3+} ($\eta = 7.05 \text{ eV}$),⁴³ Tl^+ ($\eta = 7.2 \text{ eV}$),¹³ U^{4+} ($\eta = 7.4 \text{ eV}$),⁴⁴ and Ni^{2+} ($\eta = 8.5 \text{ eV}$),¹³ some of which are radioactive. Additionally, noble gases evolved in the off-gas during nuclear fuel reprocessing⁴⁵ could, in theory, be selectively captured with chalcogels based on their high polarizabilities ($\alpha \times 10^{-24} \text{ cm}^3$), i.e., ^{85}Kr ($\alpha = 2.484$) and Xe ($\alpha = 4.044$),^{46,47} as compared to the lower polarizabilities of the surrounding species, that is, N_2 ($\alpha = 1.74$),^{46,48} NO ($\alpha = 1.7$),⁴⁹ O_2 ($\alpha = 1.57$),⁵⁰ and H_2 ($\alpha = 0.81$).⁴⁶ However, this would likely require subambient or even cryogenic temperatures, which might prove difficult to implement in a reprocessing facility. One of the other gaseous species of interest evolved during reprocessing is ^{14}C in the form of $^{14}\text{CO}_2$, which has a high polarizability ($\alpha = 2.91$),⁵¹ is considered a soft Lewis acid ($\eta = 6.9 \text{ eV}$),¹³ and has been demonstrated to adsorb to Pt-based chalcogels⁷ as was discussed previously.

3.6. Environmental Implications of Chalcogels Sorbents. Our study clearly indicated that chalcogels assembled with various building blocks can be used to remove gaseous iodine (or radioactive ^{129}I) and aqueous radionuclides (^{99}Tc and ^{238}U). Furthermore, the wide range of high capture

efficiencies for various radionuclides with all polarities as discussed here implies that chalcogels can be potentially considered as a versatile sorbent in many different applications where the species of interest is a soft acid or more polarizable than the surrounding secondary species. For example, chalcogels would be a candidate sorbent as a backfill barrier material in underground radioactive waste repositories to prevent potential leaching of radioactive contaminants because of their inherent high capture capacity for different phases of radioactive contaminants.

One concern with these sorbents is the toxicity associated with some of the chalcogel constituents such as Se, Te, Pb, and Cr, a few of which are controlled by the EPA under the Resource Conservation and Recovery Act.⁵² However, many chalcogel chemistries do not include these toxic elements. Also, some of these compounds show moderate to high air sensitivity that has been observed to increase with the progression S → Se → Te. However, with a few exceptions,⁹ most of the research to date shows that sulfide-based chalcogels are quite stable in air and when submersed in water. Additionally, research is currently underway to assess the difference between the binding affinity of S- and Se-based chalcogels of like chemistry for iodine and the details of that study will be presented in a subsequent paper.

ASSOCIATED CONTENT

Supporting Information

Experimental details regarding the chemicals used to fabricate the chalcogels in this study as well as the parameters for aging, solvent exchange, and supercritical drying. This material is available free of charge via the Internet at <http://pubs.acs.org/>.

AUTHOR INFORMATION

Corresponding Author

*Phone: (509) 372-4651; e-mail: brian.riley@pnnl.gov.

Notes

The authors declare no competing financial interest.

ACKNOWLEDGMENTS

The Pacific Northwest National Laboratory is operated by Battelle under Contract Number DE-AC05-76RL01830. Authors thank John McCloy and Denis Strachan for helpful review of this document. We thank Naoki Kikuchi at JEOL Ltd. for providing SEM micrographs of the uncoated chalcogels. This work was funded in part by the Department of Energy Office of Nuclear Energy and in part by an internal Laboratory-Directed Research and Development project. A portion of this research was supported by WCU (World Class University) program at Pohang University of Science and Technology (POSTECH) through the National Research Foundation of Korea funded by the Ministry of Education, Science, and Technology (R31-30005). Research on chalcogels and radionuclide capture at Northwestern University is funded by the Department of Energy's Nuclear Energy University Partnership program.

REFERENCES

- Kanatzidis, M. G. Beyond silica: nonoxidic mesostructured materials. *Adv. Mater.* **2007**, *19* (9), 1165.
- Kalebaila, K. K.; Georgiev, D. G.; Brock, S. L. Synthesis and characterization of germanium sulfide aerogels. *J. Non-Cryst. Solids* **2006**, *352* (3), 232.

- (3) Mohanan, J. L.; Arachchige, I. U.; Brock, S. L. Porous semiconductor chalcogenide aerogels. *Science* **2005**, *307* (5708), 397.
- (4) Bag, S.; Trikalitis, P. N.; Chupas, P. J.; Armatas, G. S.; Kanatzidis, M. G. Porous semiconducting gels and aerogels from chalcogenide clusters. *Science* **2007**, *317* (5837), 490.
- (5) Kanatzidis, M. G.; Bag, S. Semiconducting aerogels from chalcogenido clusters with broad applications, U.S. patent 2008/0241050 A1, Northwestern University, 2008, p 10.
- (6) Bag, S.; Gaudette, A. F.; Bussell, M. E.; Kanatzidis, M. G. Spongy chalcogels of non-platinum metals act as effective hydrodesulfurization catalysts. *Nat. Chem.* **2009**, *1* (3), 217.
- (7) Bag, S.; Kanatzidis, M. G. Chalcogels: Porous metal-chalcogenide networks from main-group metal ions. Effect of surface polarizability on selectivity in gas separation. *J. Am. Chem. Soc.* **2010**, *132* (42), 14951.
- (8) Shafeei-Fallah, M.; Alexander, R.; Katsoulidis, A. P.; He, J.; Malliakas, C. D.; Kanatzidis, M. G. Extraordinary selectivity of $\text{CoMo}_3\text{S}_{13}$ chalcogel for C_2H_6 and CO_2 adsorption. *Adv. Mater.* **2011**, *23* (42), 4857.
- (9) Polychronopoulou, K.; Malliakas, C.; He, J.; Kanatzidis, M. Selective surfaces: Quaternary $\text{Co}(\text{Ni})\text{MoS}$ -based chalcogels with divalent (Pb^{2+} , Cd^{2+} , Pd^{2+}) and trivalent (Cr^{3+} , Bi^{3+}) metals for gas separation. *Chem. Mater.* **2012**, *24* (17), 3380.
- (10) Oh, Y.; Bag, S.; Malliakas, C. D.; Kanatzidis, M. G. Selective surfaces: High-surface-area zinc tin sulfide chalcogels. *Chem. Mater.* **2011**, *23* (9), 2447.
- (11) Riley, B. J.; Chun, J.; Ryan, J. V.; Matyáš, J.; Li, X. S.; Matson, D. W.; Sundaram, S. K.; Strachan, D. M.; Vienna, J. D. Chalcogen-based aerogels as a multifunctional platform for remediation of radioactive iodine. *RSC Adv.* **2011**, *1*, 1704.
- (12) Pala, I. R.; Brock, S. L. ZnS nanoparticle gels for remediation of Pb^{2+} and Hg^{2+} polluted water. *ACS Appl. Mater. Interfaces* **2012**, *4* (4), 2160.
- (13) Parr, R. G.; Pearson, R. G. Absolute hardness: companion parameter to absolute electronegativity. *J. Am. Chem. Soc.* **1983**, *105* (26), 7512.
- (14) Pearson, R. G. Hard and soft acids and bases. *J. Am. Chem. Soc.* **1963**, *85* (22), 3533.
- (15) Pearson, R. G. *Chemical Hardness*; Wiley-VCH Verlag GmbH: Weinheim, Germany, 1997.
- (16) *Environmental Radiation Protection Requirements for Normal Operations of Activities in the Uranium Fuel Cycle*, 40 CFR 190; Environmental Protection Agency: Washington, D.C., 2012.
- (17) *Standards for Protection against Radiation*, 10 CFR 20; United States Nuclear Regulatory Commission: Washington, D.C., 2012.
- (18) Um, W.; Chang, H.-S.; Lechner, J. P.; Lukens, W. W.; Serne, R. J.; Qafoku, N. P.; Westsik, J. H.; Buck, E. C.; Smith, S. C. Immobilization of 99-technetium (VII) by Fe(II)-goethite and limited reoxidation. *Environ. Sci. Technol.* **2011**, *45* (11), 4904.
- (19) Um, W.; Serne, R.; Wang, Z.; Brown, C.; Williams, B.; Dodge, C.; Francis, A. Uranium phases in contaminated sediments below Hanford's U tank farm. *Environ. Sci. Technol.* **2009**, *43* (12), 4280.
- (20) Wahlquist, D. L.; Bateman, K. J.; Westphal, B. R. Second generation experimental equipment design to support voloxidation testing at INL. In *Proceedings of 16th International Conference on Nuclear Engineering*; Vol. 2, p91.
- (21) *Radioactivity in the Terrestrial Environment*; Shaw, G., Ed.; Elsevier: Oxford, UK, 2007; Vol. 10.
- (22) Collins, J. L.; Egan, B. Z.; Anderson, K. K.; Chase, C. W.; Bell, J. T. In *2nd International Conference of Waste Management: Challenges and Innovations in the Management of Hazardous Waste*, CONF-9505101-1; Washington, D.C., 1995; p 1.
- (23) Gu, B.; Dowlen, K. E.; Liang, L.; Clausen, J. L. Efficient separation and recovery of technetium-99 from contaminated groundwater. *Sep. Technol.* **1996**, *6* (2), 123.
- (24) Kohlickova, M.; Jedinakova-Krizova, V.; Horejs, M. Influence of technetium and rhenium speciation on the sorption on natural sorbents. *Czech. J. Phys.* **1999**, *49* (1), 695.
- (25) Matyáš, J.; Fryxell, G. E.; Busche, B. J.; Wallace, K.; Fifield, L. S. In *Ceramic Engineering and Science: Ceramic Materials for Energy Applications*; Lin, H.-T., Katoh, Y., Fox, K. M., Belharouak, I., Widjaja, S., Singh, D., Eds.; Wiley-The American Ceramic Society: Daytona Beach, FL, 2011; Vol. 32, p 23.
- (26) Watanabe, Y.; Ikoma, T.; Yamada, H.; Suetsugu, Y.; Komatsu, Y.; Stevens, G. W.; Moriyoshi, Y.; Tanaka, J. *Novel Long-Term Immobilization Method for Radioactive Iodine-129 Using a Zeolite/Apatite Composite Sintered Body* **2009**, *1* (7), 1579.
- (27) Sava, D. F.; Rodriguez, M. A.; Chapman, K. W.; Chupas, P. J.; Greathouse, J. A.; Crozier, P. S.; Nenoff, T. M. Capture of volatile iodine, a gaseous fission product, by zeolitic imidazolate framework-8. *J. Am. Chem. Soc.* **2011**, *133* (32), 12398.
- (28) Katsoulidis, A. P.; He, J.; Kanatzidis, M. G. Functional monolithic polymeric organic framework aerogel as reducing and hosting media for Ag nanoparticles and application in capturing of iodine vapors. *Chem. Mater.* **2012**, *24* (10), 1937.
- (29) Haefner, D. R.; Tranter, T. J. *Methods of Gas Phase Capture of Iodine from Fuel Reprocessing Off-Gas: A Literature Survey*, INL/EXT-07-12299; Idaho National Laboratory, 2007.
- (30) Um, W.; Mattigod, S.; Serne, R.; Fryxell, G.; Kim, D.; Troyer, L. Synthesis of nanoporous zirconium oxophosphate and application for removal of U(VI). *Water Res.* **2007**, *41* (15), 3217.
- (31) Ryan, J.; Buck, E.; Chun, J.; Crum, J.; Riley, B.; Strachan, D.; Sundaram, S.; Turo, L.; Vienna, J. *Alternate Waste Forms: Aqueous Processing*, AFCI-WAST-PMO-MI-DV-2009-000360; Pacific Northwest National Laboratory: Richland, WA, 2009.
- (32) Michard, P.; Guibal, E.; Vincent, T.; Le Cloirec, P. Sorption and desorption of uranyl ions by silica gel: pH, particle size and porosity effects. *Microporous Mater.* **1996**, *5* (5), 309.
- (33) Coleman, S. J.; Coronado, P. R.; Maxwell, R. S.; Reynolds, J. G. Granulated activated carbon modified with hydrophobic silica aerogel-potential composite materials for the removal of uranium from aqueous solutions. *Environ. Sci. Technol.* **2003**, *37* (10), 2286.
- (34) Woignier, T.; Reynes, J.; Phalippou, J.; Dussossoy, J. L.; Jacquart-Francillon, N. N. Sintered silica aerogel: a host matrix for long life nuclear wastes. *J. Non-Cryst. Solids* **1998**, *225* (1), 353.
- (35) Manos, M. J.; Kanatzidis, M. G. Layered metal sulfides capture uranium from seawater. *J. Am. Chem. Soc.* **2012**, *134* (39), 16441.
- (36) Krebs, V. B.; Pohl, S.; Schiwy, W. Darstellung und Struktur von $\text{Na}_4\text{Ge}_2\text{S}_6 \cdot 14\text{H}_2\text{O}$ und $\text{Na}_4\text{Sn}_2\text{S}_6 \cdot 14\text{H}_2\text{O}$. *Z. Anorg. Allg. Chem.* **1972**, *393* (3), 241.
- (37) Bowes, C. L.; Huynh, W. U.; Kirkby, S. J.; Malek, A.; Ozin, G. A.; Petrov, S.; Twardowski, M.; Young, D. Dimetal linked open frameworks: $[(\text{CH}_3)_4\text{N}]_2(\text{Ag}_2,\text{Cu}_2)\text{Ge}_4\text{S}_{10}$. *Chem. Mater.* **1996**, *8* (8), 2147.
- (38) Brunauer, S.; Emmett, P. H.; Teller, E. Adsorption of gases in multimolecular layers. *J. Am. Chem. Soc.* **1938**, *60* (2), 309.
- (39) Gregg, S.; Sing, K. *Adsorption, Surface Area, And Porosity*; 2nd ed.; Academic Press: Orlando, 1982.
- (40) Preetha, C. R.; Gladis, J. M.; Rao, T. P.; Venkateswaran, G. Removal of toxic uranium from synthetic nuclear power reactor effluents using uranyl ion imprinted polymer particles. *Environ. Sci. Technol.* **2006**, *40* (9), 3070.
- (41) Walter, M.; Arnold, T.; Reich, T.; Bernhard, G. Sorption of uranium(VI) onto ferric oxides in sulfate-rich acid waters. *Environ. Sci. Technol.* **2003**, *37* (13), 2898.
- (42) Um, W.; Serne, R.; Krupka, K. Surface complexation modeling of U(VI) adsorption to Hanford sediment with varying geochemical conditions. *Environ. Sci. Technol.* **2007**, *41* (10), 3587.
- (43) Cotton, S. *Lanthanide and Actinide Chemistry, Inorganic Chemistry: A Textbook Series*; John Wiley & Sons, Ltd.: West Sussex, 2006.
- (44) Pyper, N. C.; Grant, I. P. Studies in multiconfiguration Dirac-Fock theory III. Interpretation of the electronic structure of neutral and ionized states of uranium. *J. Chem. Soc., Faraday Trans. 2* **1978**, *74* (11), 1885.
- (45) Paviet-Hartmann, P.; Kerlin, W.; Bakhtiar, S. *Treatment of Gaseous Effluents Issued from Recycling—A Review of the Current*

Practices and Prospective Improvements, INL/CON-10-19961; Idaho National Laboratory, 2010.

(46) Orcutt, R. H.; Cole, R. H. Dielectric constants of imperfect gases. III. Atomic gases, hydrogen, and nitrogen. *J. Chem. Phys.* **1967**, *46* (2), 697.

(47) Miller, T. M.; Bederson, B. Atomic and molecular polarizabilities—A review of recent advances, In *Advances in Atomic and Molecular Physics*; Bates, D. R., Benjamin, B., Eds.; Academic Press: New York, 1978; Vol. 13, p 1.

(48) Newell, A. C.; Baird, R. C. Absolute determination of refractive indices of gases at 47.7 gigahertz. *J. Appl. Phys.* **1965**, *36* (12), 3751.

(49) Maryott, A. A.; Buckley, F. *Circular of the Bureau of Standards: Table of Dielectric Constants and Electric Dipole Moments of Substances in the Gaseous State*; U.S. Dept. of Commerce, National Bureau of Standards, 1953; Vol. 537.

(50) May, E. F.; Moldover, M. R.; Schmidt, J. W. Electric and magnetic susceptibilities of gaseous oxygen: Present data and modern theory compared. *Phys. Rev. A* **2008**, *78* (3), 032522.

(51) Bose, T. K.; Cole, R. H. Dielectric and pressure virial coefficients of imperfect gases. II. CO₂–argon mixtures. *J. Chem. Phys.* **1970**, *52* (1), 140.

(52) *Identification and Listing of Hazardous Waste*, CFR 261; Environmental Protection Agency: Washington, D.C., 2012; Vol. 40.